# Coordination Strategies for Securing AC/DC Flexible Transmission Networks With Renewables

Yanfei Chen, Rodrigo Moreno, *Member, IEEE*, Goran Strbac, *Member, IEEE*, and Diego Alvarado

***Abstract*—This paper studies key aspects of preventive and corrective security strategies to coordinate flexible transmission network infrastructure. To do so, we propose a two-stage stochastic optimization model that can efficiently coordinate available preventive and corrective control actions (pre- and post-contingency) from flexible network technologies, generation, and demand, while explicitly considering the likelihood of postcontingency events and wind/solar uncertainty. This stochastic/probabilistic model constitutes the counterfactual against which current deterministic, preventive operational practices are compared. Flexible network equipment such as HVDC and FACTS devices are efficiently modeled through a tight MILP representation and network losses are also included through a linear representation. Through several case studies, we demonstrate the advantages of probabilistic, corrective security to improve coordination of HVDC and FACTS setpoints and thus reduce network congestion and reserve holding levels, improving the overall efficiency of the system operation. We also quantify the value loss associated with current deterministic, preventive control operational practices when coordinating setpoints of flexible network equipment, demonstrating that adding flexible network technology could even increase system costs under a preventive security approach.**

***Index Terms*—Transmission network operation, FACTS, HVDC, preventive security, corrective network security, power system economics.**

## NOMENCLATURE

*A. Parameters (written in normal font)*

| | |
|---|---|
| $a_k, b_k, c_k$ | Three parameters to calculate converter losses of DC line k ($a_k$ in MW and $b_k, c_k$ in p.u.). |
| $A_{l,s}$ | Availability of AC line l in state s (binary). |
| $A_{k,s}$ | Availability of DC line k in state s (binary). |
| $A_{g,s}$ | Availability of generator g in state s (binary in case of outages and continuous in case of forecast errors). |
| $d_n$ | Demand in node n [MW]. |
| $\bar{f}_l$ | Capacity of (AC or DC) line l [MW]. |
| $\bar{f}_l^{AC}$ | Capacity of AC line l [MW]. |
| $\underline{f}_k^{DC}, \bar{f}_k^{DC}$ | Minimum and maximum capacity of DC line k [MW]. |
| $h_{l,n,s}$ | Power transfer distribution factor (PTDF) of line l and node n in state s [p.u.]. |
| $M_{l,s}$ | Constant value to apply disjunctive approach on series compensation in line l in state s [MW]. |
| $\underline{p}_g, \bar{p}_g$ | Minimum and maximum allowed power output of generator g [MW]. |
| $r_l$ | Resistance of line l [p.u.]. |
| $X_l^{AC}$ | Reactance of AC line l [p.u.]. |
| $\underline{X}_l^{SC}, \bar{X}_l^{SC}$ | Minimum and maximum reactance of series compensator in line l [p.u.]. |
| $\alpha_{l,s,p}$ | Slope of piecewise approximation of network losses associated with line l in state s in segment p [p.u.]. |
| $\underline{\delta}, \bar{\delta}$ | Generic minimum and maximum reactance of a FACTS device[%]. |
| $\Delta f_l$ | Power flow step used in the piecewise function of network losses associated with line l [MW]. |
| $\underline{\theta}_l^{QB}, \bar{\theta}_l^{QB}$ | Minimum and maximum voltage angle of quad-booster transformer in line l [rad]. |
| $\rho_s$ | Probability of occurrence of state s [p.u.]. |

*B. Variables (written in italic font)*

| | |
|---|---|
| $f_{l,s}$ | Power flow in line l in state s [MW]. |
| $f_{l,s}^+, f_{l,s}^-$ | Power flow in line l in state s: positive and negative contribution, respectively [MW]. |
| $f_{l,s}^{AC}$ | Power flow (including FACTS devices contribution) in AC line l in state s [MW]. |
| $\hat{f}_{l,s}^{AC}$ | Power flow in AC line l in state s (without contribution from potential FACTS device installed in line l) [MW]. |
| $f_{k,s}^{DC}$ | Power flow in DC line k in state s [MW]. |
| $\hat{f}_{l,s}^{FACTS}$ | Power flow contribution of FACTS device installed in line l in state s [MW]. |
| $f_{l,s,p}^{piece}$ | Power flow of line l in state s associated with segment p (used in piecewise approximation of network losses) [MW]. |
| $I_{g,s}$ | Intertrip of generator g in state s (binary). |
| $ll_{n,s}$ | Lost load (demand side response) in node n in state s [MW]. |
| $Mf_{l,s}$ | Power flow in absolute value of line l in state s [MW]. |

Manuscript received August 9, 2017; revised April 21, 2018; accepted June 11, 2018. Date of publication June 28, 2018; date of current version October 18, 2018. The work of R. Moreno was supported by the Complex Engineering Systems Institute (CONICYT-PIA-FB0816; ICM P-05-004-F), and the Conicyt-Chile under Grants Fondecyt/1181928, Newton-Picarte/MR/N026721/1, and SERC Fondap/15110019. The work of D. Alvarado was supported by Conicyt project PFCHA/MagísterNacional/2017-22171423. The work of G. Strbac was supported by EPSRC project ACCEPT EP/K036173/1. Paper no. TPWRS-01242-2017. *(Corresponding author: Rodrigo Moreno.)*

Y. Chen and G. Strbac are with the Department of Electrical and Electronic Engineering, Imperial College, London SW7 2AZ, U.K. (e-mail: yanfei.chen11@imperial.ac.uk; g.strbac@ imperial.ac.uk).

R. Moreno is with the Universidad de Chile, Santiago 1058, Chile, and also with the Imperial College, London SW7 2AZ, U.K. (e-mail: rmorenovieyra@ing.uchile.cl).

D. Alvarado is with the Universidad de Chile, Santiago 1058, Chile (e-mail: diego.alvarado@ing.uchile.cl).

Digital Object Identifier 10.1109/TPWRS.2018.2851214

$p_g$ Power output of generator g in the pre-fault condition [MW].
$r_g^{up}$ Holding volume of up reserve services provided by generator g [MW].
$r_g^{dw}$ Holding volume of downward reserve services provided by generator g. This also accounts for cost of intertrip. [MW].
$TL_{l,s}$ Thermal losses of line l in state s [MW].
$TL_{l,s}^{AC}$ Thermal losses of AC line l in state s [MW].
$TL_{k,s}^{Cable}$ Thermal losses associated with the cable of DC line k in state s [MW].
$TL_{k,s}^{Converter}$ Thermal losses associated with the converter of DC line k in state s [MW].
$TL_{k,s}^{DC}$ Thermal losses (including converter losses) of DC line k in state s [MW].
$X_{l,s}^{FACTS}$ Reactance of FACTS device in line l in state s [p.u.].
$Y_{l,s}$ Binary variable to apply disjunctive approach on series compensator in line l in state s (binary).
$\gamma_g$ Commitment status of generator g (same pre and post-fault unless unit is tripped) (binary).
$\Delta p_{g,s}$ Power output change of generator g from pre to post-fault state s [MW].
$\omega_{k,s}$. Commitment status of DC line k in state s (binary).

*C. Set and related constants (written in italic font)*

$G$ Set of generators.
$G_n$ Set of generators in node n.
$L$ Set of all AC and DC lines.
$L^{AC}$ Set of AC lines (with and without FACTS devices).
$L^{DC}$ Set of DC lines.
$L^{FACTS}$ Set of lines with FACTS devices.
$L^{QB}$ Set of lines with quad-booster transformers.
$L^{SC}$ Set of lines with series compensators.
$N$ Set of nodes.
$P$ Set of segments in linear piecewise representation of network losses.
$S$ Set of states (intact system and contingencies).
$S^G$ Set of generation contingencies/states.
$from_y$ Node from which network component y is connected.
$to_y$ Node to which network component y is connected.

*D. Functions (written in bold font)*

$\mathbf{C_g^{G.Pre}}(\cdot)$ Cost function of generator g during pre-contingency state [$].
$\mathbf{C_{g,s}^{G.Post}}(\cdot)$ Cost function of generator g during post-contingency state s [$].
$\mathbf{C_{n,s}^{D.Post}}(\cdot)$ Cost function of demand side response in node n in state s [$].
$\mathbf{h_{l,n,s}}(\cdot)$ Power transfer distribution factor (PTDF) function of line l and node n in state s [p.u.].
$\mathbf{TL_{l,s}^{AC}}(\cdot)$ Thermal losses (non-linear) function of AC line l in state s [MW].
$\mathbf{TL_{k,s}^{DC}}(\cdot)$ Thermal losses (non-linear) function of DC line k in state s [MW].

## I. Introduction

FLEXIBLE transmission systems such as FACTS and HVDC can support a more economically efficient and reliable network operation through increased power flow controllability, releasing latent network capacity to users from existing infrastructure [1]. In fact, active control of flexible network devices can alleviate congestions without the need for asset-heavy network investment solutions (e.g., new lines and transformers), increasing the utilization levels of the existing infrastructure and consequently supporting integration of renewable generation in a more efficient and expeditious fashion [2]–[4]. Moreover, increased generation reserves, that are needed to deal with renewables' uncertain and variable outputs in real time, can be more efficiently located and accessed in real time if network equipment setpoints can be rapidly controlled and co-optimized with generation outputs [5], [6]. In addition, the role of network redundancy to provide security of supply can be, at least in part, displaced by the active control of network equipment that can rapidly respond to eliminate post-contingency overloads due to generation outages, realization of large wind/solar forecast errors, and network infrastructure outages [6]. Increased network utilization through optimal use of flexible network equipment, however, may present some downsides such as exposure to potentially larger thermal losses and risks associated with the exercise of demand and generation curtailments that have to be properly quantified and balanced against the corresponding benefits.

Currently, although FACTS and HVDC are being increasingly adopted in power networks around the world, there are several operational practices that impede their efficient utilization. Firstly, setpoints of flexible network devices are rarely modified in real time [5], which, together with the preventive approach to network security of system operators, undermines the value of flexibility. Secondly, the deterministic approach to security that considers reliability as a binary feature where the system is, for a given operating condition and set of operational decisions, either secured or not (i.e., if it meets the N-k criterion), is biased and favors redundancy and asset-heavy solutions [7]. In reality, system reliability is, of course, not binary and this could be even enhanced when FACTS and HVDC are preferred over network redundancy levels and this has to be properly measured and understood. Thirdly, complexity associated with computational tools and mathematical programs prevent optimization of FACTS and HVDC setpoints within security constraints unit commitment, optimal power flow and market clearing/economic dispatch models [8].

Furthermore, it is important to emphasize that even in the case without FACTS and HVDC equipment, security constrained and probabilistic/stochastic optimal power flow (OPF) type problems remain a challenge and therefore we need a number of simplifying assumptions to make them tractable [9]. Assumptions made need to be aligned with the objectives of the targeted studies. In this vein, linearized security/risk constrained DC OPF type models have been developed, although –for some applications– these are questioned since these fundamentally ignore thermal losses and reactive power (e.g., [7], [10], [11]). On the other hand, risk based security constrained AC OPF type

models have been also proposed such as that in [12], notwithstanding that the limited number of contingent states that can be analyzed within the optimization framework may become problematic for some studies. Reference [9] offers a comprehensive literature review in the area of security and risk constrained operational models, discussing their key simplifications.

In the area of operation of flexible devices, several papers have proposed novel optimization models and demonstrated the benefits of flexible network technology in power systems with both conventional and renewable generation [2], [4]–[6], [8], [13]–[22]. The current state of the art has reported benefits in terms of congestion management [2], [4]–[6], [8], [13]–[17], losses management [4], [14], [15], reliability and security enhancements [4], [6], [8], [13], [14], [16], [18]–[22], stability improvements [4], renewable curtailment minimization [2], [4]–[6], [8], [13], [14], reserves deliverability [6], [13], [14], [16], and investment deferrals [16]. To do so, both AC and DC OPF type models have been developed. While representation of HVDC is relatively straightforward in DC-OPF models (see, for instance, [4]), references [5], [13] explain the non-linear nature of FACTS setpoints optimization (even in a DC-OPF fashion) and propose an exact representation of FACTS through a mixed integer linear programming (MILP) model that uses disjunctive, big-M constraints to treat FACTS devices and hence eliminate the non-linear equations.

Expanding on this, we develop an enhanced MILP 2-stage stochastic model that includes network losses and a number of contingent states (combining outages and forecast errors) so as to coordinate an array of network devices, generation outputs and special protection schemes for generation and demand curtailments in a DC power flow framework. Through this model, we attempt to quantify the economic and reliability benefits of FACTS and HVDC real-time control with probabilistic security as opposite to the current preventive and deterministic approach to operational security.

The true value of HVDC and FACTS equipment in the context of renewables (and from a static, steady-state perspective) lays on the higher levels of controllability that allows system operators to efficiently manage pre- and post-contingency network congestions, minimize network losses (this is particularly important in the presence of HVDC links due to extra losses in converter stations), minimize demand curtailment, optimize the utilization of generation reserves in real time, etc. Hence, we investigate how different strategies to coordinate network equipment can affect the value of FACTS and HVDC with a special focus on current practices and its value loss in the renewable generation context with respect to a counterfactual case, where a 2-stage stochastic optimization model (also called probabilistic model) is used to efficiently coordinate all possible pre- and post-contingency actions from generation and network devices and protection schemes (including FACTS, HVDC and SPS for generation tripping and demand side response), considering a comprehensive set of post-contingency states (beyond credible N-1 events, including changes in wind/solar outputs). Our model balances pre-contingency, first-stage generation costs associated with units' outputs and reserve capacity held, against those incurred during post-contingency (in expected value), including expected costs of reserve utilization, and generation and demand curtailments (that can be significant). Solutions from this counterfactual model can be compared against current deterministic, preventive control operational practice in order to assess its value loss. In this context, our contributions are:

- Quantify the value loss associated with current deterministic, preventive control operational practices when coordinating HVDC and FACTS setpoints with renewables.
- Illustrate the interactions among post-contingency, real-time coordination of FACTS and HVDC, network congestion and generation reserves, demonstrating that:
  - optimal and coordinated use of flexible network equipment can significantly reduce reserve levels without degrading reliability.
  - installation of flexible network equipment can, paradoxically, increase rather than decrease operational costs under current deterministic, preventive control operational practices in some conditions.
- Develop an optimization model suitable for offline analysis that:
  - coordinates in a probabilistic fashion pre- and post-contingency control variables (generation outputs, reserves, demand side response, and generation tripping through SPS combined with setpoints of FACTS devices and HVDC), including (linearized) network losses through AC and DC network infrastructure (i.e., cables and converters), and (linearized) power flows equations (i.e., DC power flow model).
  - represents FACTS devices more efficiently through a tight representation, where value of big-M parameters are minimized.

Although advances in AC and DC flexible transmission network equipment are vast and have been rapidly progressing lately as previously explained, to our knowledge, this is the first study (with the abovementioned characteristics) that fundamentally compares different network security strategies (from preventive and deterministic security to corrective and probabilistic security) in terms of the coordination of AC and DC flexible equipment, explaining in detail the associated operational impacts on cost efficiency and reliability in an electricity system with renewables (considering a large number of possible states, combining outages and forecast errors).

This paper is organized as follows. Section III formulates our modelling framework, while Sections IV and V demonstrate the advantages of the corrective, probabilistic security strategy through two examples. Section VI discusses the computational performance of our probabilistic modelling approach. Section VII concludes.

## II. Assessment Methodology

### A. Overview

Our methodology seeks to determine optimal network operation and quantify its associated costs and risks, and hence this is composed of an (i) MILP module that determines optimal network operation and a (ii) risk assessment (or out-of-sample) module that calculates the expected costs (including that of en-

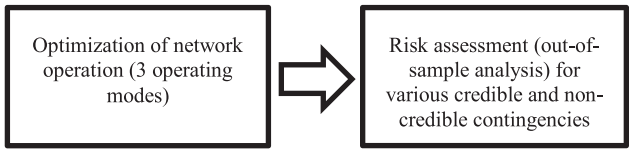


Fig. 1. Overview of the proposed assessment methodology.

ergy not supplied) for various contingent states, including scenarios of generation and network outages (beyond N-1 events) as well as wind/solar forecast errors (and their combinations).

The first module corresponds to a 2-stage stochastic optimization model that coordinates pre- and post-contingency decisions (in the first and second stage, respectively) at the generation (including energy, holding and utilization of reserves, and tripping actions through SPS), network (FACTS and HVDC setpoints) and demand (curtailments) levels. This module minimizes overall operating costs while ensuring that generation outputs and network loads are within capacity limits. This module can be run in 3 modes as follows:

1. *Preventive mode (with deterministic security):* This ignores the possibility to carry out post-contingency control except for generation reserves that are used under generation outages and wind/solar changes and thus network operation has to be secured through network redundancy only (i.e., network congestion) against a set of credible contingencies. Due to the absence of reliability information (in particular, outage probabilities), the model minimizes pre-contingency costs only.
2. *Corrective mode with deterministic security:* This coordinates pre- and post-contingency control actions in the generation and flexible AC/DC network infrastructure (while demand curtailments are not allowed), providing security through a portfolio of preventive and corrective measures. As in the preventive mode, only credible contingencies are modelled. Due to the absence of reliability information (in particular, outage probabilities), the model minimizes pre-contingency costs only.
3. *Corrective mode with probabilistic security:* This fully coordinates all possible pre- and post-contingency actions from generation, network and demand, considering a comprehensive set of post-contingency states (beyond credible N-1 events) and their probabilities. Under this mode, the model minimizes pre- and post-contingency costs.

The second module corresponds to an optimization program that determines the optimal network response after a contingency occurs, for a given pre-contingency dispatch condition. The objective function minimizes the post-contingency costs. Fig. 1 summarizes our 2-module assessment methodology that is used to study the economic and reliability performance of the three aforementioned operating modes.

### *B. First Module: Optimization of AC/DC Network Operation in Probabilistic Security Mode*

First, in this Section III-B we will describe the model under the corrective control mode with probabilistic security since this represents the most complex and complete mathematical formulation of those above described (the other two modes are variants and thus they can be modelled by a similar set of equations and this will be explained later on in Section III-C). In turn, Section III-B is divided into four parts. Section III-B1 presents the compact (non-linear) formulation to optimize pre- and post-contingency control of flexible AC/DC network components in coordination with further actions from generation and demand (including curtailments of both through SPS) with probabilistic security. We call it the *compact model* since equations associated with FACTS and losses are presented through generic, compact functions. We present first the model in a compact manner so as to ease and facilitate the understanding of our proposal, which is further developed and completed in the following sections, taking the compact model as a starting point. Note that although this model is based on linearized, DC power flow equations, the compact model is non-linear due to the presence of FACTS equipment and thermal losses. Consequently, Section III-B2 develops the disjunctive, big-M equations associated with FACTS so as to treat them in an MILP fashion. Importantly, we propose a formula to determine optimal big-M values per FACTS device in order to efficiently run the optimization model. Section III-B3 presents a linearization of network losses, including those associated with HVDC cables and converters that present both a fixed and a variable component. Finally, for the sake of completeness Section III-B4 briefly presents a scenarios-selection method (previously developed in [7]) to run the stochastic optimization model in a more efficient manner.

*1) The Compact Non-Linear AC/DC Network Model:* The model minimizes system costs (during pre- and post-contingency) associated with generation dispatches, holding and utilization levels of reserves, and generation and demand curtailments as shown in Eq. (1). The supply-demand-losses balance for all states (including pre- and post-contingency) is shown in Eq. (2), where $\mathbf{TL}_{\boldsymbol{l,s}}^{\boldsymbol{AC}}(\cdot)$ and $\mathbf{TL}_{\boldsymbol{l,s}}^{\boldsymbol{DC}}(\cdot)$ are non-linear functions that represent thermal losses. Eqs. (3), (4) limit pre and post-contingency outputs of generating units according to generation capacity, reserve holding levels and intertripping actions (where the latter is treated through a disjunctive approach; note that the asymmetry of Eq. (4) is needed to relax the lower bound of $\Delta p_{g,s}$ when a unit is tripped), while Eq. (5) constrains demand curtailments. Eqs. (6)–(8) represent the power flow constraints where AC (rather than DC) transfers depend on network reactances. Note that Eq. (8) is non-linear since PTDF functions $\mathbf{h}_{\boldsymbol{l,n,s}}(\cdot)$ change with controllable FACTS setpoints and are multiplied by net nodal injections (nodal production minus demand, where HVDC links can contribute through positive and negative nodal injections; here we chose to use PTDF structure due to its computational advantages as indicated in [4], [8]), and Eq. (9) limits the compensation level associated with FACTS.

$$\text{Min}\left\{\sum_{g\in G}\mathbf{C}_{\boldsymbol{g}}^{\boldsymbol{G.Pre}}\left(p_g,\gamma_g,r_g^{up},r_g^{dw}\right)+\sum_{s\in S}\rho_s\left[\sum_{g\in G}\mathbf{C}_{\boldsymbol{g,s}}^{\boldsymbol{G.Post}}\left(\Delta p_{g,s},I_{g,s}\right)+\sum_{n\in N}\mathbf{C}_{\boldsymbol{n,s}}^{\boldsymbol{D.Post}}\left(ll_{n,s}\right)\right]\right\} \quad (1)$$

s.t.

$$\sum_{g\in G} p_g + \sum_{g\in G} \Delta p_{g,s} = \sum_{n\in N} \left(\mathrm{d}_n - ll_{n,s}\right) + \sum_{l\in L^{AC}} \mathbf{TL}^{\boldsymbol{AC}}_{\boldsymbol{l,s}}(f^{AC}_{l,s}) + \sum_{k\in L^{DC}} \mathbf{TL}^{\boldsymbol{DC}}_{\boldsymbol{k,s}}(f^{DC}_{k,s}) \quad \forall s\in S \tag{2}$$

$$\underline{p}_g \cdot A_{g,s} \cdot \left(\gamma_g - I_{g,s}\right) \le p_g + \Delta p_{g,s} \le \bar{p}_g \cdot A_{g,s} \cdot \left(\gamma_g - I_{g,s}\right) \quad \forall g\in G, \forall s\in S \tag{3}$$

$$-\bar{p}_g \cdot (1 - A_{g,s} + I_{g,s}) - r^{dw}_g \le \Delta p_{g,s} \le r^{up}_g \quad \forall g\in G, \forall s\in S \tag{4}$$

$$ll_{n,s} \le \mathrm{d_n} \quad \forall n\in N, \forall s\in S \tag{5}$$

$$-\bar{f}^{AC}_l \cdot A_{l,s} \le f^{AC}_{l,s} \le \bar{f}^{AC}_l \cdot A_{l,s} \quad \forall l\in L^{AC}, \forall s\in S \tag{6}$$

$$-\bar{f}^{DC}_k \cdot A_{k,s} \le f^{DC}_{k,s} \le \bar{f}^{DC}_k \cdot A_{k,s} \quad \forall k\in L^{DC}, \forall s\in S \tag{7}$$

$$f^{AC}_{l,s} = \sum_{n\in N} \mathbf{h_{l,n,s}}\left(\mathrm{X}^{AC}_l, X^{FACTS}_{l,s}\right) \cdot \left( \sum_{g\in G_n} p_g + \sum_{g\in G_n} \Delta p_{g,s} - \left(\mathrm{d}_n - ll_{n,s}\right) + \sum_{k\in L^{DC}|\mathrm{to_k}=\mathrm{n}} f^{DC}_k - \sum_{k\in L^{DC}|from_k=n} f^{DC}_k \right) \quad \forall l\in L^{AC},\ \forall s\in S \tag{8}$$

$$\underline{\delta}\cdot \mathrm{X}^{AC}_l \le X^{FACTS}_{l,s} \le \bar{\delta}\cdot \mathrm{X}^{AC}_l \ \forall l\in L^{FACTS}, \forall s\in S \tag{9}$$

$$p_g, r^{up}_g, r^{dw}_g \in \mathbb{R}^+ \quad \forall g\in G;\ ll_{n,s}\in\mathbb{R}^+ \quad \forall n\in N, \forall s\in S;$$
$$\gamma_g \in \{0,1\} \quad \forall g\in G;\ I_{g,s} \in \{0,1\} \quad \forall g\in G, \forall s\in S;$$
$$\Delta p_{g,s}\in\mathbb{R} \quad \forall g\in G, \forall s\in S;\ \ f^{AC}_{l,s}, X^{FACTS}_{l,s}\in\mathbb{R}$$
$$\forall l\in L^{AC}, \forall s\in S;\ f^{DC}_{k,s} \in \mathbb{R} \quad \forall k\in L^{DC}, \forall s\in S \tag{10}$$

*2) FACTS Devices Modeling in a MILP Fashion:* The power injection model developed in [23] suggests isolating power flow contribution from FACTS devices as shown in Eq. (11). This power flow decomposition allows us to represent power flow contributions from FACTS devices such as quad-booster (phase-shifter) transformers (QB) and series compensation (SC) as shown in Eq. (12), (13), where the "if" statement (associated with SC) can be treated through a disjunctive, big-M approach and this will be explained in the next section. Finally, Eq. (14) corresponds to the power flow equation when considering the contributions from FACTS in net nodal injections. Note that while $\hat{f}^{AC}_{l,s}$ are state variables driven by net nodal injections and fixed network impedances (without FACTS), $\hat{f}^{FACTS}_{l,s}$ are fully controllable within the ranges indicated in Eq. (12)-(13) (as the thyristor controlled series capacitors –TCSC– presented in [4]). In Eq. (14), PTDFs (represented by $h_{l,n,s}$) are constant values rather than a function of variable FACTS' reactances as in Eq. (8).

$$-\bar{f}^{AC}_l \le f^{AC}_{l,s} = \hat{f}^{AC}_{l,s} + \hat{f}^{FACTS}_{l,s} \le \bar{f}^{AC}_l \quad \forall l\in L^{FACTS}, \forall s\in S \tag{11}$$

$$\underline{\theta}^{QB}_l / X^{AC}_l \le \hat{f}^{FACTS}_{l,s} \le \bar{\theta}^{QB}_l / X^{AC}_l \quad \forall l\in L^{QB}, \forall s\in S \tag{12}$$

if $\hat{f}^{AC}_{l,s} \ge 0$

$$-\left(\frac{\bar{X}^{SC}_l}{X^{AC}_l + \bar{X}^{SC}_l}\right)\cdot \hat{f}^{AC}_{l,s} \le \hat{f}^{FACTS}_{l,s} \le -\left(\frac{\underline{X}^{SC}_l}{X^{AC}_l + \underline{X}^{SC}_l}\right)\cdot \hat{f}^{AC}_{l,s} \quad \forall l\in L^{SC}, \forall s\in S \tag{13a}$$

if $\hat{f}^{AC}_{l,s} < 0$

$$-\left(\frac{\underline{X}^{SC}_l}{\mathrm{X}^{AC}_l + \underline{\mathrm{X}}^{SC}_l}\right)\cdot \hat{f}^{AC}_{l,s} \le \hat{f}^{FACTS}_{l,s} \le -\left(\frac{\bar{\mathrm{X}}^{SC}_l}{\mathrm{X}^{AC}_l + \bar{\mathrm{X}}^{SC}_l}\right)\cdot \hat{f}^{AC}_{l,s} \quad \forall l\in L^{SC}, \forall s\in S \tag{13b}$$

$$\hat{f}^{AC}_{l,s} = \sum_{n\in N} h_{l,n,s}\cdot\Bigg(\sum_{g\in G_n} p_g + \sum_{g\in G_n}\Delta p_{g,s} - \left(d_n - ll_{n,s}\right) + \sum_{j\in L^{FACTS}|to_j=n} \hat{f}^{FACTS}_{j,s} - \sum_{j\in L^{FACTS}|from_j=n} \hat{f}^{FACTS}_{j,s} + \sum_{k\in L^{DC}|to_k=n} f^{DC}_{k,s} - \sum_{k\in L^{DC}|from_k=n} f^{DC}_{k,s}\Bigg) \forall l\in L^{AC},\ \forall s\in S \tag{14}$$

*a) The Tighter Big-M Formulation:* References [5], [13] developed big-M representation of Eq. (13), allowing us to optimize FACTS setpoints by an MILP model and this is shown in Eq. (15), where the big-M formulation has been adapted to our power injection model of FACTS that isolates the power flow contribution of FACTS devices in the term $\hat{f}^{FACTS}_{l,s}$.

$$-Y_{l,s}\cdot M_{l,s} - \left(\frac{\bar{X}^{SC}_l}{X^{AC}_l + \bar{X}^{SC}_l}\right)\cdot \hat{f}^{AC}_{l,s} \le \hat{f}^{FACTS}_{l,s} \le -\left(\frac{\underline{X}^{SC}_l}{X^{AC}_l + \underline{X}^{SC}_l}\right)\cdot \hat{f}^{AC}_{l,s} + Y_{l,s}\cdot M_{l,s} \quad \forall l\in L^{SC}, \forall s\in S \tag{15a}$$

$$-(1-Y_{l,s})\cdot \mathrm{M}_{l,s} - \left(\frac{\underline{\mathrm{X}}^{SC}_l}{\mathrm{X}^{AC}_l + \underline{\mathrm{X}}^{SC}_l}\right)\cdot \hat{f}^{AC}_{l,s} \le \hat{f}^{FACTS}_{l,s} \le -\left(\frac{\bar{\mathrm{X}}^{SC}_l}{\mathrm{X}^{AC}_l + \bar{\mathrm{X}}^{SC}_l}\right)\cdot \hat{f}^{AC}_{l,s} + (1-Y_{l,s}) \cdot \mathrm{M}_{l,s} \quad \forall l\in L^{SC}, \forall s\in S \tag{15b}$$

$$Y_{l,s}\in\{0,1\} \quad \forall l\in L^{SC}, \forall s\in S \tag{16}$$

Note that (by definition) either Eq. (15a) or (15b) will be enforced at the time depending on the value of $Y_{l,s}$ (that represents the direction of $\hat{f}^{AC}_{l,s}$ and is binary according to Eq. (16)), which means that the lower and upper bounds associated with Eq.(15a) should be tighter than those of Eq.(15b) when $Y_{l,s} = 0$ and vice versa. Consequently, the minimum value of M (marked with $*$)

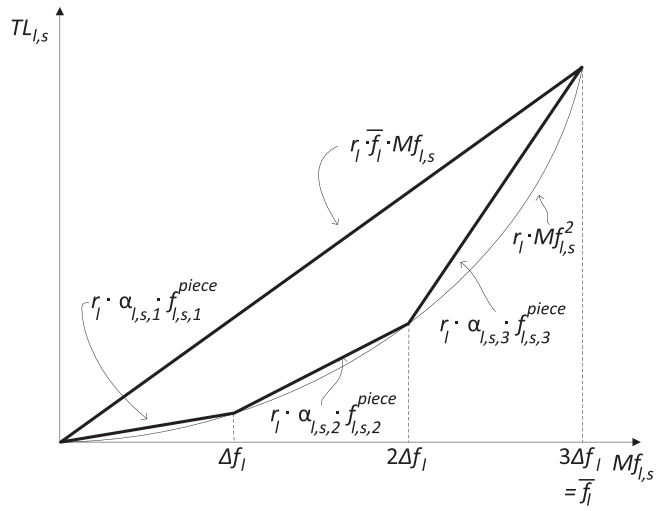


Fig. 2. Losses approximation through 3 segments or pieces that act as lower bounds (the number of segments can be, evidently, increased for higher accuracy) and an upper bound. Thicker lines indicate the ultimate searching space. Ideally, a lower bound should be binding due to penalization of losses in the objective function.

must comply with Eq. (17).

$$M_{l,s}^{*} = \left[\left(\frac{\underline{X}_l^{SC}}{X_l^{AC} + \underline{X}_l^{SC}}\right) - \left(\frac{\bar{X}_l^{SC}}{X_l^{AC} + \bar{X}_l^{SC}}\right)\right] \cdot \max\left|\hat{f}_{l,s}^{AC}\right| \quad \forall l \in L^{SC}, \forall s \in S \tag{17}$$

Furthermore, if we define (for simplicity) a symmetric compensation level $\delta$ such that $\bar{X}_l^{SC} = -\delta \cdot X_l^{AC}$ and $\underline{X}_l^{SC} = \delta \cdot X_l^{AC}$, and replace $\max|\hat{f}_{l,s}^{AC}| = \bar{f}_l^{AC} \cdot (1+\delta)$, then Eq. (17) can be re-written as Eq. (18), where subscript 's' disappears.

$$M_l^{*} = \frac{2\delta}{(1-\delta)} \cdot \bar{f}_l^{AC} \quad \forall l \in L^{SC} \tag{18}$$

*3) Linear Representation of Network Losses:*

*a) AC/DC conductor/cable losses:* We adopted a similar representation of thermal losses as that in [24] through Eq. (19)–(23), which fundamentally approximates the quadratic losses function through a piecewise linear representation as shown in Fig. 2. Particularly, Eq. (19) relates each power transfer with two positive auxiliary variables used in Eq. (20) to determine the absolute values of power transfers (we do so in order to eliminate the need to define more variables associated with another piecewise approximation over negative power flows). Eq. (21)–(23) approximate the quadratic losses function through segments or pieces (where $\alpha_{l,s,p}$ is the slope of piece $p$). Note that Eq. (23) should use piece $p$ to calculate losses only if Eq. (22) is binding for previous pieces $p-1, p-2, \ldots, 1$. As there is no constraint enforcing this requirement, the approximation may lead to disproportionally higher losses. In this line, reference [25] proposes the use of binary variables to eliminate this problem, however this significantly increases computational burden that we attempt to minimize in our model. So, we propose adding Eq. (24) as an upper bound (see Fig. 2). We also further penalize losses in the objective function every time we observe a disproportionally higher amount of losses in our results. In our case studies discussed later on, the natural penalization of losses in our model (since losses increase demand and therefore costs) is sufficient to make this approximation work properly.

$$f_{l,s} = f_{l,s}^{+} - f_{l,s}^{-} \quad \forall l \in L, \forall s \in S \tag{19}$$

$$Mf_{l,s} = f_{l,s}^{+} + f_{l,s}^{-} \quad \forall l \in L, \forall s \in S \tag{20}$$

$$Mf_{l,s} = \sum_{p \epsilon P} f_{l,s,p}^{piece} \quad \forall l \in L, \forall s \in S \tag{21}$$

$$f_{l,s,p}^{piece} \leq \Delta f_l \quad \forall l \in L, \forall s \in S, \forall p \in P \tag{22}$$

$$TL_{l,s} = \sum_{p \epsilon P} \mathrm{r}_l \cdot \alpha_{l,s,p} \cdot f_{l,s,p}^{piece} \quad \forall l \in L, \forall s \in S \tag{23}$$

$$TL_{l,s} \leq r_l \cdot \bar{f}_l \cdot Mf_{l,s} \quad \forall l \in L, \forall s \in S \tag{24}$$

$$f_{l,s}^{+}, f_{l,s}^{-}, Mf_{l,s}, TL_{l,s} \in \mathbb{R}^{+} \quad \forall l \in L, \forall s \in S; f_{l,s,p}^{piece} \in \mathbb{R}^{+} \quad \forall l \in L, \forall s \in S, \forall p \in P; f_{l,s} \in \mathbb{R} \quad \forall l \in L, \forall s \in S \tag{25}$$

Eqs.(19)–(25) are applied on AC and DC lines, and since losses in a line are allocated to its end nodes –one half each– as additional demand, we need to re-write Eq. (14) as Eq. (26).

$$\begin{aligned}\hat{f}_{l,s}^{AC} = & \sum_{n \in N} h_{l,n,s} \cdot \Bigg( \sum_{g \in G_n} p_g + \sum_{g \in G_n} \Delta p_{g,s} - (d_n - ll_{n,s}) \\ & + \sum_{j \in L^{FACTS} | to_j = n} \hat{f}_{j,s}^{FACTS} \\ & - \sum_{j \in L^{FACTS} | from_j = n} \hat{f}_{j,s}^{FACTS} + \sum_{k \in L^{DC} | to_k = n} f_{k,s}^{DC} \\ & - \sum_{k \in L^{DC} | from_k = n} f_{k,s}^{DC} - \sum_{l \in L^{AC} | to_l = n} \frac{TL_{l,s}^{AC}}{2} \\ & - \sum_{l \in L^{AC} | from_l = n} \frac{TL_{l,s}^{AC}}{2} - \sum_{k \in L^{DC} | to_k = n} \frac{TL_{k,s}^{DC}}{2} \\ & - \sum_{k \in L^{DC} | from_k = n} \frac{TL_{k,s}^{DC}}{2} \Bigg) \forall l \in L^{AC}, \forall s \in S \end{aligned} \tag{26}$$

*b) DC converter losses:* We split HVDC cable and converter losses as shown in Eq. (27) and, following [26], add three types of losses components that are present in converter stations: (i) non-load losses, (ii) linear losses and (iii) quadratic losses, shown in Eq. (28). Furthermore, we use the values suggested in [26] for a typical VSC-HVDC link of 600 MW and ±300 kV DC, which are $a_l = 13.2$, $b_l = 0.0058$ and $c_l = 0.0000125$ (these values are adapted to capacity of each HVDC link and this accounts for the total losses from 2 converter stations). Note that we use the same piecewise linear representation illustrated in Fig. 2 to approximate the quadratic part of $TL_{k,s}^{DC}$ (i.e., $TL_{k,s}^{Cable}$ and $TL_{k,s}^{Converter}$). Additionally, Eq. (29), (30) ensures that non-load losses are positive only when converter stations are working (where $\underline{f}_k^{DC}$ is a very small positive number).

$$TL_{k,s}^{DC} = TL_{k,s}^{Cable} + TL_{k,s}^{Converter} \quad \forall k \in L^{DC}, \forall s \in S \tag{27}$$

$$TL_{k,s}^{Converter} = \mathrm{a}_k \cdot \omega_{k,s} + \mathrm{b}_k \cdot Mf_{k,s} + \sum_{p \epsilon P} \mathrm{c}_k \cdot \alpha_{k,s,p} \cdot f_{k,s,p}^{piece}$$

$$\forall k \in L^{DC}, \forall s \in S \tag{28}$$

$$\underline{f}_k^{DC} \cdot \omega_{k,s} \leq Mf_{k,s} \leq \bar{f}_k^{DC} \cdot \omega_{k,s} \quad \forall k \in L^{DC}, \forall s \in S \tag{29}$$

$$\omega_{k,s} \in \{0,1\} \quad \forall k \in L^{DC}, \forall s \in S \tag{30}$$

*4) Umbrella States Identification:* According to [27], the set of umbrella contingencies in a probabilistic assessment is a subset of the full set of all contingencies that is sufficient to attain levels of security and economic performance that is very close to the one obtained when all contingencies are considered. Hence identifying umbrella states is paramount to run the probabilistic model efficiently and we do so through implementing the method described in [7].

### C. First Module: Optimization of AC/DC Network Operation in Deterministic Security Modes

*1) Corrective Mode:* To determine a deterministic solution of the operational problem with corrective security, we modify the proposed probabilistic model shown in Section III-B assuming: only contingencies considered credible (N-1 outages of generation and network, and wind/solar changes equal to $\pm 3$ times the standard deviation $\sigma$ of its forecast error); all state probabilities equal to 1; price of generation-based post-fault actions approaching zero (i.e., SPS, generation re-dispatches/reserves utilization); and price of demand shedding approaching infinity (i.e., no demand shedding is allowed under the occurrence of a credible contingency). Note that no extra equations are needed with respect to those associated with the previous probabilistic model since the abovementioned changes are only in terms of input data. With these modifications, the model becomes deterministic (considering corrective mode), optimizing only the pre-contingency costs of transmission constraints and generation reserve holding for a given reliability profile, in which no rating violations and no demand shedding are permitted under the predefined set of credible events.

*2) Preventive Mode:* To determine a deterministic solution of the operational problem with preventive security, we add further constraints to the above model in Section III-C1 in order to make the value of post-contingency variables of flexible network equipment equal to their pre-contingency value as shown in Eq. (31). Generation outputs can be different pre- and post-contingency and thus reserves can be utilized only if the contingent event relates to generation and this in enforced in Eq. (32).

$$\left[X_{l,s}^{FACTS}; f_{k,s}^{DC};\ \omega_{k,s}\right] = \left[X_{l,1}^{FACTS}; f_{k,1}^{DC};\ \omega_{k,1}\right]$$
$$\forall s \in S \backslash \{s=1\},\ \forall l \in L^{FACTS}, \forall k \in L^{DC} \tag{31}$$

$$\Delta p_{g,s} = 0 \qquad \forall s \in S \backslash S^G \tag{32}$$

Note that the 2-stage stochastic model and its deterministic variants correspond to MILP models.

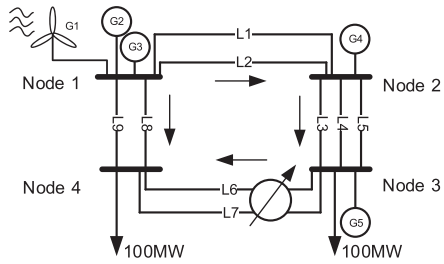


Fig. 3. 4-node system (positive flows defined by arrows).

### D. Second Module: Risk Assessment of a Given Pre-Contingency Dispatch (Out-of-Sample Analysis)

Following [7], the assessment of the expected post-fault costs associated with a given intact system dispatch is carried out by running the probabilistic operational module (over the corresponding operating condition and over a given comprehensive set of operating states) with a set of extra constraints that forces the pre-contingency output and reserve holding level of each generator and the pre-contingency setpoint of each flexible device to be equal to those from the given intact system dispatch (obtained through the application of the first module). This is enforced by Eq. (33), where optimal values of pre-contingency variables obtained in the first module are denoted by a '$*$'. The resulting post-fault cost (or *risk*) will be equal to Eq. (1) minus the pre-contingency cost. Note that this module just quantifies the expected costs associated with a given intact system dispatch (that can be obtaining by either a probabilistic or deterministic operational model) and this allows us to assess the risk levels of each AC/DC coordination strategy.

$$\left[p_g; \gamma_g; r_g^{up}; r_g^{dw}; X_{l,1}^{FACTS}; Y_{l,1} f_{k,1}^{DC};\ \omega_{k,1}\right]$$
$$= \left[p_g^*; \gamma_g^*; r_g^{up*}; r_g^{dw*}; X_{l,1}^{FACTS*}; Y_{l,1}^*; f_{k,1}^{DC*}; \omega_{k,1}^*\right]$$
$$\forall g \in G,\ \forall l \in L^{FACTS}, \forall k \in L^{DC} \tag{33}$$

## III. Small-Scale Study: Illustration, Validation, and Analysis Over a 4-Bus Network

This section studies the economic and reliability performance of the three operating modes introduced in the previous section (namely preventive with deterministic security, corrective with deterministic security, and corrective with probabilistic security) when optimizing multiple AC/DC flexible network devices in coordination with generation (and demand in the probabilistic case). We focus on transfer/congestion levels, reserve holding levels, expected energy not supplied and the value of flexibility from network devices. This small network also serves to illustrate and validate the models.

### A. Input data

Fig. 3 shows the topology of the 4-node system with 5 generators, 9 lines and 2 demands. We analyze various case studies where flexible network components such as SC, QB and HVDC will be located in lines 6 and 7. Table I shows further details of

TABLE I
4-NODES SYSTEM'S GENERATION AND NETWORK DATA

| Generator | Capacity | Minimum Generation | Ramp up/down | Fuel cost | Reserve Utilization cost | $\lambda$ |
|---|---|---|---|---|---|---|
| | MW | | | £/MWh | | occ/yr |
| G1 | 112 | 0 | 112 | 0 | *NA* | 1.8 |
| G2 | 95 | 80 | 15 | 2.8 | 2.8 | 0.3 |
| G3 | 136 | 10 | 126 | 6 | 6 | 0.3 |
| G4 | 200 | 150 | 50 | 25 | 25 | 1.8 |
| G5 | 100 | 77 | 23 | 70 | 70 | 40 |

| Lines | Rating [MW] | $\lambda$ [occ/yr] |
|---|---|---|
| L1 | 100 | 0.04 |
| L2 | 100 | 0.04 |
| L3 | 55 | 60 |
| L4 | 55 | 60 |
| L5 | 55 | 60 |
| L6 | 23 | 0.04 |
| L7 | 23 | 0.04 |
| L8 | 58 | 0.04 |
| L9 | 58 | 0.04 |

TABLE II
NORMALIZED WIND LEVELS AND THEIR PROBABILITIES

| State | 1 | 2 | 3 | 4 | 5 |
|---|---|---|---|---|---|
| Wind level [%] | 0.85 | 0.05 | 0.15 | 0.25 | 0.35 |
| Probability [p.u.] | 0.37 | 3E-4 | 5E-4 | 0.002 | 0.044 |
| State | 6 | 7 | 8 | 9 | 10 |
| Wind level [%] | 0.45 | 0.55 | 0.65 | 0.75 | 0.95 |
| Probability [p.u.] | 0.1 | 0.13 | 0.15 | 0.19 | 0.03 |

the system, where outage rates of lines 3,4,5 and generator 5 are deliberately higher.

Apart from the pre-contingency condition, we model 103 system outages (i.e., 14 N-1 outages and 89 selected N-2 outages) that are combined with 10 different wind levels, which represents a total of 1040 different states. Expected wind availability (pre-contingency) is 85%, which can be different in real-time due to forecast errors and this is shown in Table II, where different wind levels (in real-time) are associated with their probabilities (state 1, that with the higher probability, represents the expected, pre-contingency condition).

Offer and bid prices (those associated with increases and decreases of power output with respect to the unconstrained, single-node dispatch position) are equal to the fuel prices as well as the utilization prices of reserve. The reserve holding price, on the other hand, is \$2/MW/h for all units. VoLL is 30 k\$/MWh and SPS price is 200 k\$ per generating unit tripped.

Regarding FACTS capability/flexibility, SC can compensate up to $\pm 60\%$ and QB can shift up to $\pm 40°$. For HVDC, we consider a cable resistance of 0.0075 p.u. and the following parameters associated with converter losses: a = 0.092, b = 0.001 and c = 0.00006 (used in Eq. (28)). Pre- and post-fault line ratings present 2 MW difference for all lines (post-fault ratings are higher).

### B. Case Studies

We analyze 3 operating modes or control strategies and 4 different levels of flexibility in lines 6,7. The operating modes are:

A. Deterministic security with preventive control (DSP)
B. Deterministic security with corrective control (DSC)
C. Probabilistic security with corrective control (PSC)

TABLE III
GENERATOR DISPATCH IN PRE-FAULT CONDITION IN [MW]

| Control strategy | Flexibility case | G1 | G2 | G3 | G4 | G5 |
|---|---|---|---|---|---|---|
| PSC | HVDC | 95 | 95 | 15 | 0 | 0 |
| | QB | 95 | 95 | 14 | 0 | 0 |
| | SC | 95 | 95 | 14 | 0 | 0 |
| | NF | 43 | 0 | 10 | 150 | 0 |
| DSC | HVDC | 44 | 0 | 10 | 150 | 0 |
| | QB | 43 | 0 | 10 | 150 | 0 |
| | SC | 43 | 0 | 10 | 150 | 0 |
| | NF | 43 | 0 | 10 | 150 | 0 |
| DSP | HVDC | 35 | 80 | 10 | 0 | 77 |
| | QB | 43 | 0 | 10 | 150 | 0 |
| | SC | 42 | 0 | 10 | 151 | 0 |
| | NF | 36 | 0 | 10 | 156 | 0 |

TABLE IV
COST OF 3 OPERATING MODES COMBINED WITH 4 NETWORK FLEXIBILITY LEVELS IN [\$/30MIN]

| Control strategy | Costs of | HVDC | QB | SC | NF |
|---|---|---|---|---|---|
| PSC | Constraints | 13 | 12 | 12 | 2012 |
| | Reserve Hold | 95 | 95 | 95 | 158 |
| | Reserve Used | 50 | 50 | 50 | 1 |
| | SPS | 0 | 0 | 0 | 7 |
| | DSR | 26 | 26 | 30 | 34 |
| | Total | 184 | 183 | 187 | 2212 |
| DSC | Constraints | 2011 | 2012 | 2012 | 2012 |
| | Reserve Hold | 151 | 151 | 153 | 160 |
| | Reserve Used | 1 | 1 | 1 | 1 |
| | SPS | 0 | 0 | 7 | 7 |
| | DSR | 38 | 38 | 40 | 41 |
| | Total | 2201 | 2202 | 2213 | 2221 |
| DSP | Constraints | 2979 | 2020 | 2030 | 2127 |
| | Reserve Hold | 95 | 155 | 155 | 160 |
| | Reserve Used | 0 | 1 | 1 | 1 |
| | SPS | 0 | 7 | 7 | 7 |
| | DSR | 529 | 53 | 54 | 54 |
| | Total | 3603 | 2236 | 2247 | 2349 |

The 4 levels of flexibility to be analyzed are: lines 6,7 with (i) HVDC, (ii) QB, (iii) SC, and (iv) without flexible device (NF). We use Julia v0.6 and CPLEX v12.8 [28] on a server with 24 cores (Intel Xeon E5 v3) and 100 GB of RAM.

### C. Results and Discussion

Generation dispatches together with their associates costs and risks are shown in Tables III and IV, respectively. Table III shows that wind production and overall generation from node 1 (which is more economically efficient) is maximized under corrective and probabilistic security (PSC) and when the network presents flexible equipment (HVDC, QB and SC), demonstrating that the probabilistic approach truly maximizes the value of flexible network technologies. Likewise, Table IV demonstrates that both costs and risks (i.e., expected cost of demand curtailment or DSR) are the lowest under corrective and probabilistic security (PSC) and when the network presents flexible equipment (HVDC, QB and SC). This is so since the probabilistic approach explicitly balances costs and risks in the objective function and optimizes a larger set of control variables pre- and post-fault,

finding a true Pareto solution between economic and reliability performance. In this particular case, note that the probabilistic solution maximizes production from the most efficient generators in node 1 which tends to increase power transfers through lines 8 and 9 (that also present a lower outage rate) in order to ship power to loads centers in nodes 3 and 4. Deterministic solutions, instead, constrain power transfers through lines 8 and 9 (in order to meet the N-1 security criterion), which leads to wind curtailment, increased production from more costly fuel-based generators and more transfers through lines 3,4,5 which are extremely unreliable (since the deterministic approach is not sensitive to lines' outage rates, which is fundamentally inefficient).

While installation of flexible network technologies presents real economic and reliability benefits under the probabilistic security approach since equipment such as SC, QB and HVDC can significantly drop the operational costs and risks, their flexibility is not adequately utilized and valued under deterministic approaches, and remarkably, can even worsen both cost and reliability levels. For instances, installation of HVDC links in lines 6 and 7 can increase dispatch costs and risks as shown in Table IV (see cases DSP/HVDC and DSP/NF). This is so since HVDC transfers under a preventive control mode, by definition, will remain constant during pre and post-contingency (e.g., network or generation contingency). Note that, under such preventive control mode, an AC line can be proved to be more flexible than an HVDC line in terms of accommodating post-contingency transfers as the former will naturally transfer different amounts of power during pre- and post-fault conditions due to changes in the network's admittance matrix (driven by network faults) and/or changes in net injections (driven by generation events and reserve utilization). On the contrary, in the HVDC case the preventive control mode will force pre- and post-fault transfers to be equal through the HVDC line (regardless of the fault occurred), potentially degrading both the economic and reliability performance of the solution. Moreover, in our particular case, transfers through HVDC line must remain constant (under the preventive control mode) even under major outages (e.g., line 3 or 4 or 5), causing a drop in the power amounts that can be securely transferred pre-fault from nodes 1,2 to nodes 3,4.

Regarding the number of states utilized, remarkably, we can demonstrate that the initial 1040 states can be reduced to less than 100 states in the probabilistic model (the exact number depends on the particular case study) without significantly affecting the optimal solution (cost difference according to Eq. (1) with all initial states and the reduced set of states is less than 0.5%) and this is possible because the "umbrella" outages (those that drive the optimal decision) can be identified without the need to run the optimization with the entire set of initial outages as explained in [7].

## IV. IEEE-RTS Study: Costs, Risks and Reserve Levels

This section analyzes the economic and reliability performance and the use of generation reserves under various probabilistic and deterministic operating modes or strategies to coordinate AC/DC network infrastructure in a larger-scale transmission network.

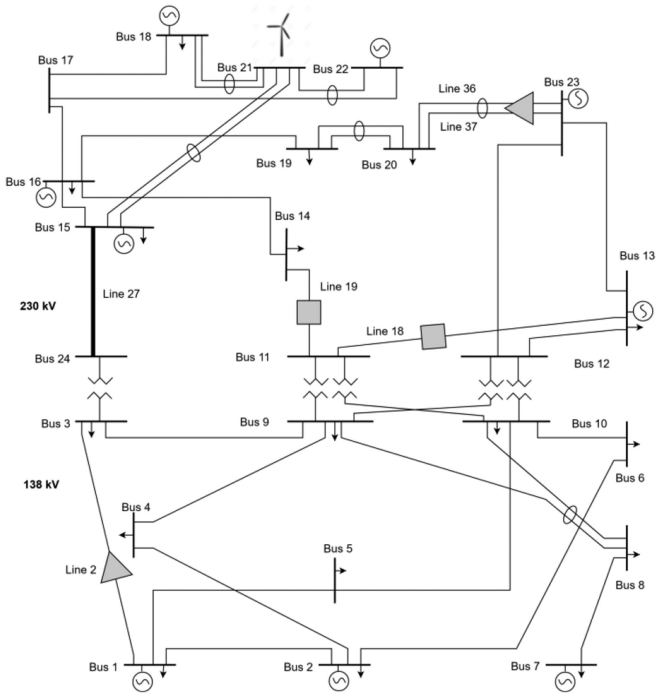


Fig. 4. 24-busbar IEEE-RTS topology. Triangles refer to QBs, squares refer to SC and thicker line refers to HVDC.

### A. Input Data

We modified the IEEE RTS described in [29] by adding:

a) 340-MW and 200-MW demand in nodes 9 and 10.
b) two 250-MW generating units in nodes 16 and 23.
c) three 350-MW wind generators in node 21.
d) one 400-MW HVDC link in line 27.
e) two SCs with $\pm 30\%$ compensation capacity in lines 18 and 19.
f) three QBs with $\pm 40°$ shifting capacity in lines 2, 36, 37.

The above changes are illustrated in Fig. 4. Note that a)-c) are aimed to increase network transfers and d)-f) to add flexibility to the network. Relevant cost and reliability data is taken from [7], [29], [30] where VoLL is equal to 1 k$/MWh, the SPS utilization cost (i.e., generation curtailment) is equal to 7 k$ per unit tripped (no availability cost), and the reserve holding cost is equal to 15$/MW/h. Post-fault line ratings are 25% higher than those pre-fault. Outage rates are those presented in [29].

In the probabilistic model, all N-1 outages are modelled together with selected N-2 outages in combination with 10 different wind levels, totalizing 1170 states (including the intact system condition). By identifying the umbrella states, we can reduce the number of states to only 122 and maintain 1% accuracy in our results.

In the deterministic mode, only 3 wind conditions where modelled considering one expected or forecast scenario (i.e., $\mu$ equivalent to 75% wind availability) and two extreme scenarios of high ($\mu + 3\sigma$ equivalent to 85%) and low ($\mu - 3\sigma$ equivalent

TABLE V
COSTS OF 4 OPERATING MODES OR STRATEGIES IN [$/30MIN]

| Cost of | PSC | DSC | DSP | PSC* |
|---|---|---|---|---|
| Constraints | 24742 | 29600 | 45707 | 26451 |
| Reserves | 4322 | 7175 | 7587 | 5849 |
| SPS | 0 | 0 | 1 | 0 |
| DSR | 592 | 14 | 62 | 14 |
| Total | 29656 | 36789 | 53357 | 32314 |

TABLE VI
RESERVE HOLDING LEVELS IN [MW]

| | PSC | DSC | DSP | PSC* |
|---|---|---|---|---|
| Reserve holding | 576 | 957 | 1010 | 780 |

to 15%) wind outputs, which are combined with N-1 network and generation outages.

### B. Results

Table V shows the costs and risks associated with network operation under 4 different operating modes, namely, deterministic security with preventive control (DSP), deterministic security with corrective control (DSC), and probabilistic security with corrective control (PSC). We added a new probabilistic mode (PSC$*$, with respect to previous Section IV), where we limit the amount of demand curtailment to be equal to that observed under the DSC mode.

Interestingly, PSC presents the lowest costs since both pre- and post-fault operational measures are fully optimized, including generation outputs, HVDC and FACTS setpoints and demand side response. In fact, DSR cost is the highest under the probabilistic mode and this permits to disproportionally decrease the cost of constraints and reserves since DSR can be used to both balance system frequency after a generation imbalance (displacing the need for generation reserves) and eliminate post-fault network congestion (displacing the need to maintain network capacity margins/redundancy in the pre-fault condition, i.e., displacing the need for network congestion during pre-fault conditions). In addition, DSP presents the highest costs since (i) network flexibility from HVDC and FACTS cannot be fully utilized as network setpoints are forced to be fixed from pre- to post-fault, (ii) generation cannot be re-dispatched under network outages and (iii) DSR is not allowed under credible events.

Furthermore, under the DSP mode, reserves can be only accessed after an outage occurs if appropriate network margins/redundancy are scheduled in advance so as to handle post-contingency power flows due to reserve utilization. Under corrective mode, instead, reserves can be accessed by re-routing power flows through post-contingency control of HVDC and FACTS setpoints. Moreover, under the probabilistic approach, reserves holding levels can be significantly dropped without the need to use higher levels of DSR as shown in Tables V and VI, where PSC$*$ mode is such that DSR volumes are those of the deterministic, corrective security solution (DSC).

It is important to mention that this larger-scale case study cannot be solved if larger big-M values were used (ignoring Eq. (18)), the umbrella states were not identified, and binary variables were used for network losses (optimization processes were interrupted after running for an entire day), which demonstrate the advantages of our proposed model. This is explored further in the next section.

## V. 118-BUSBAR SYSTEM STUDY: COMPUTATIONAL PERFORMANCE

This section discusses the computational performance of our proposal with a particular focus on the efficient values of big-M parameters and the number of umbrella contingent states/events that are needed to run our probabilistic optimization.

### A. Input Data

We modified the IEEE 118-busbar system described in [31] by adding:

a) three 100-MW wind plants in nodes 15, 17, and 31.
b) three 100-MW solar plants in nodes 49, 69, and 80.
c) two 500-MW HVDC links in lines 51 and 90.
d) five SCs with $\pm$35% compensation capacity in lines 12, 13, 78, 97, and 100.
e) five QBs with $\pm$30° shifting capacity in lines 71, 101, 103, 133, and 135.

As in our previous case studies, relevant cost data is taken from [29] and, in this case, the VoLL is equal to 1 k$/MWh. Importantly, all N-1 outages are modelled in combination with 25 different scenarios that represent the combined forecast errors of wind and solar resources in 2 areas (we cluster and select 25 representative discrete values for the combined forecast errors assuming no correlation between wind and solar resources; these values were calculated following actual practices of the Chilean system operator [32], using a standard deviation of 13% and 8% for wind and solar power output forecast errors, respectively, during the peak demand hour; note that discussion on forecasting and clustering methods used to elaborate the set of contingent scenarios falls out of the scope of this paper), totalizing 6176 states (including the intact system condition). Outage rates are 0.1% occ/h for generators and 0.0057% occ/h for 100-km lines. Expected wind and solar availabilities (pre-contingency) are 60% and 50% respectively, which can be different in real-time due to the aforementioned forecast errors.

### B. Results

Table VII shows the results for two different numbers of umbrella states, corresponding to 1.2% and 0.5% accuracies. Interestingly, this demonstrates, once again and in line with previous developments in [7], that a highly accurate solution can be found by a significantly small number of critical, umbrella states. In fact, in our case 2.6% of the states drive 99.5% of the total costs. Importantly, we additionally found that the problem could not be solved considering the original 6176 states in the optimization (after 2 hours, we stopped the optimization solver which presented no feasible solutions found). This demonstrates the importance of scenarios-selection techniques, as that introduced in Section III-B4, particularly in this AC/DC coordination problem.

TABLE VII
RESULTS FOR DIFFERENT NUMBERS OF UMBRELLA STATES

| | Case A | Case B |
|---|---|---|
| No. of umbrella states | 120 | 163 |
| Execution time [s] | 503 | 1365 |
| Optimization cost function*[$/30min] | 18144 | 18214 |
| Out-of-sample cost* [$/30min] | 227 | 93 |
| Total cost [$/30min] | 18371 | 18307 |
| Accuracy | 1.2% | 0.5% |

*Optimization and out-of-sample costs correspond to the cost obtained directly from the optimization problem (including pre-fault cost and expected post-fault costs of umbrella states) and the expected post-fault costs of the non-umbrella states, respectively.

TABLE VIII
EFFECTS OF BIG-M VALUES ON EXECUTION TIMES

| big-M approach | Execution time [s] |
|---|---|
| Proposed, minimum big-M per FACTS | 503 |
| Highest minimum big-M, uniform* | 1577 |
| big-M = 1000, uniform | 1989 |
| big-M = 2000, uniform | 2862 |

∗Our approach (fully applied in the first row) determines one specific big-M value per FACTS device. In the second row, we use the highest minimum big-M value of those used in the first row (and equal to 539) for all FACTS devices (i.e., we use a *uniform* value).

However, the above efficiencies are not only due to the application of a scenarios-selection method. A critical contribution in terms of computational efficiency corresponds to formula (18), which derives the minimum value of a FACTS's big-M parameter to be used in our proposed mathematical program. As explained in [28], big-M values play a critical role in execution times of optimization models due to ill conditioning. In this vein, Table VIII shows the execution times of our model for different big-M values, where clearly our proposal significantly outperforms the other tests.

## VI. CONCLUSION

We studied key aspects of preventive and corrective security strategies to coordinate flexible transmission network infrastructure such as HVDC and FACTS devices, demonstrating that preventive security can significantly constrain flexible network technology to efficiently accommodate renewable generation and reduce system costs. Moreover, we demonstrated that, in some cases, adding flexible network technology could even increase system costs under a preventive security approach. We also demonstrated that HVDC and FACTS setpoints can be more efficiently coordinated with further pre- and post-contingency actions from generation and demand under a probabilistic and corrective approach, reducing the need for network redundancy/congestion and increased generation reserve levels.

We proposed an efficient optimization model that can handle a very large number of network states, determining pre- and post-contingency setpoints of HVDC and FACTS. Our MILP model combines a tight representation of FACTS, the identification of umbrella states and a piecewise linear representation of network losses (without binary variables). Further work includes expansion to an AC OPF framework like that in [4], [34] since –depending on the network– HVDC and FACTS might significantly affect voltage profiles. Another branch of further research includes implementation of decomposition methods [35] so as to further improve the computational performance of our models.

## REFERENCES


[1] D. Retzmann and K. Uecker, "Benefits of HVDC & FACTS for sustainability and security of power supply," in *Proc. Powerafrica Conf. Expo.*, Johannesburg, South Africa, 2007, pp. 1–22.

[2] F. B. Alhasawi and J. V. Milanovic, "Techno-economic contribution of FACTS devices to the operation of power systems with high level of wind power integration," *IEEE Trans. Power Syst.*, vol. 27, no. 3, pp. 1414–1421, Aug. 2012.

[3] M. E. Montilla-Djesus, D. Santos-Martin, S. Arnaltes, and E. D. Castronuovo, "Optimal operation of offshore wind farms with line-commutated HVDC link connection," *IEEE Trans. Energy Conver.*, vol. 25, no. 2, pp. 504–513, Jun. 2010.

[4] Y. Pipelzadeh, R. Moreno, B. Chaudhuri, G. Strbac, and T. C. Green "Corrective control with transient assistive measures: Value assessment for Great Britain transmission system%," *IEEE Trans. Power Syst*, vol. 32, no. 2, pp. 1638–1650, Mar. 2017.

[5] M. Sahraei-Ardakani and K. W. Hedman, "A fast LP approach for enhanced utilization of variable impedance based FACTS devices," *IEEE Trans. Power Syst.*, vol. 31, no. 3, pp. 2204–2213, May 2016.

[6] R. Moreno, Y. Chen, and G. Strbac, "Evaluation of benefits of coordinated DC & AC flexible transmission systems with probabilistic security and corrective control," in *Proc. IET Int. Conf. Resilience Transmiss. Distrib. Netw.*, Birmingham, U.K., 2015, pp. 1–6.

[7] R. Moreno, D. Pudjianto, and G. Strbac, "Transmission network investment with probabilistic security and corrective control," *IEEE Trans. Power Syst.*, vol. 28, no. 4, pp. 3935–3944, Nov. 2013.

[8] M. Sahraei-Ardakani and K. W. Hedman, "Computationally efficient adjustment of FACTS set points in DC optimal power flow with shift factor structure," *IEEE Trans. Power Sys.*, vol. 32, no. 3, pp. 1733–1740, May 2017.

[9] F. Capitanescu *et al.*, "State-of-the-art, challenges, and future trends in security constrained optimal power flow," *Elect. Power Syst. Res.*, vol. 81, no. 8, pp. 1731–1741, 2011.

[10] E. Karangelos and L. Wehenkel, "Probabilistic reliability management approach and criteria for power system real-time operation," in *Proc. Power Syst.Comput. Conf.*, Genoa, Italy, 2016, pp. 1–9.

[11] E. Karangelos, P. Panciatici, and L. Wehenkel, "Whither probabilistic security management for real-time operation of power systems?," in *Proc. Bulk Power Syst. Dyn. Control-IX Optim., Security Control Emerg. Power Grid*, Rethymnon, Crete, Greece, 2013, pp. 1–17.

[12] F. Capitanescu, "Enhanced risk-based SCOPF formulation balancing operation cost and expected voluntary load shedding," *Elect. Power Syst. Res.*, vol. 128, pp. 151–155, 2015.

[13] M. Sahraei-Ardakani and K. W. Hedman, "Day-ahead corrective adjustment of FACTS reactance: A linear programming approach," *IEEE Trans. Power Syst.*, vol. 31, no. 4, pp. 2867–2875, Jul. 2016.

[14] A. Nasri, A. J. Conejo, S. J. Kazempour, and M. Ghandhari, "Minimizing wind power spillage using an OPF with FACTS devices," *IEEE Trans. Power Syst.*, vol. 29, no. 5, pp. 2150–2159, Sep. 2014.

[15] S. Y. Ge and T. S. Chung, "Optimal active power flow incorporating power flow control needs in flexible AC transmission systems," *IEEE Trans. Power Syst.*, vol. 14, no. 2, pp. 738–744, May 1999.

[16] A. Moreira, G. Strbac, R. Moreno, A. Street, and I. Konstantelos, "A Five-Level MILP model for flexible transmission network planning under uncertainty: A min-max regret approach," *IEEE Trans. Power Syst.*, vol. 33, no. 1, pp. 486–501, Jan. 2018.

[17] P. G. Thakurta, R. Belmans, and D. Van Hertem, "Risk-based management of overloads caused by power injection uncertainties using power flow controlling devices," *IEEE Trans. Power Syst.*, vol. 30, no. 6, pp. 3082–3092, Nov. 2015.

[18] J. Cao, W. Du, and H. F. Wang "An improved corrective security constrained OPF for meshed AC/DC grids with multi-terminal VSC-HVDC," *IEEE Trans. Power Syst.*, vol. 31, no. 1, pp. 485–495, Jan. 2016.

[19] R. Yang and G. Hug-Glanzmann, "Regression-based corrective power flow control for system risk minimization," in *Proc. IEEE Power Energy Soc. General Meeting*, Vancouver, Canada, 2013, pp. 1–5.

[20] G. Hug, "Generation cost and system risk trade-off with corrective power flow control," in *Proc. Commun., Control, Comput.*, Allerton, IL, USA, 2012, pp. 1324–1331.
[21] J. Mohammadi, G. Hug, and S. Kar, "A benders decomposition approach to corrective security constrained OPF with power flow control devices," in *Proc. IEEE Power Energy Soc. General Meeting*, Vancouver, Canada, 2013, pp. 1–5.
[22] M. Sahraei-Ardakani and K. W. Hedman, "Day-ahead corrective adjustment of FACTS reactance: A linear programming approach," *IEEE Trans. Power Syst.*, vol. 31, no. 4, pp. 2867–2875, Jul. 2016.
[23] M. Noroozian and G. Andersson, "Power flow control by use of controllable series components," *IEEE Trans. Power Deli.*, vol. 8, no. 3, pp. 1420–1429, Jul. 1993.
[24] H. Zhang, V. Vittal, G. T. Heydt, and J. Quintero, "A mixed-integer linear programming approach for multi-stage security-constrained transmission expansion planning," *IEEE Trans. Power Syst.*, vol. 27, no. 2, pp. 1125–1133, May 2012.
[25] N. Alguacil, A. L. Motto, and A. J. Conejo, "Transmission expansion planning: A mixed-integer LP approach," *IEEE Trans. Power Syst.*, vol. 18, no. 3, pp. 1070–1077, Aug. 2003.
[26] G. Daelemans, K. Srivastava, M. Reza, S. Cole, and R. Belmans, "Minimization of steady-state losses in meshed networks using VSC HVDC," in *Proc. IEEE Power Energy Soc. General Meeting*, 2009, pp. 1–5.
[27] F. Bouffard, F. D. Galiana, and J. M. Arroyo, "Umbrella contingencies in security-constrained optimal power flow," in *Proc. Power Syst. Comput. Conf.*, Liege, Belgium, 2005, pp. 1–7.
[28] The Julia Language, 2017. [Online]. Available: https://julialang.org/.
[29] Reliability Test System Task Force, "The IEEE reliability test system—1996%," *IEEE Trans. Power Syst.*, vol. 14, no. 3, pp. 1010–1020, Aug. 1999.
[30] F. Bouffard, F. D. Galiana, and A. Conejo, "Market-clearing with stochastic security—Part II: Case studies," *IEEE Trans. Power Syst.*, vol. 20, no. 4, pp. 1827–1835, Nov. 2005.
[31] University of Washington, "Power systems test case archive," May 1993. [Online]. Available: https://www2.ee.washington.edu/research/pstca/. Accessed on: Apr. 16th, 2018.
[32] A. Inzunza, R. Moreno, A. Bernales, and H. Rudnick "CVaR constrained planning of renewable generation with consideration of system inertial response, reserve services and demand participation," *Energy Econo.*, vol. 59, pp. 104–117, 2016.
[33] L. Bahiense, G. C. Oliveira, M. Pereira, and S. Granville, "A mixed integer disjunctive model for transmission network expansion," *IEEE Trans. Power Syst.*, vol. 16, no. 3, pp. 560–565, Aug. 2001.
[34] P. Henneaux and D. S. Kirschen, "Probabilistic security analysis of optimal transmission switching," *IEEE Trans. Power Syst.*, vol. 31, no. 1, pp. 508–517, Jan. 2016.
[35] A. J. Conejo, E. Castillo, R. Minguez, and R. Garcia-Bertrand, *Decomposition Techniques in Mathematical Programming: Engineering and Science Applications*. New York, NY, USA: Springer, 2006.

**Yanfei Chen** received the B.Sc. degree in electrical engineering from Northumbria University, Newcastle upon Tyne, U.K., in 2011, and the M.Sc. and Ph.D. degrees in electrical engineering from the Imperial College, London, U.K., in 2012 and 2017, respectively. He is currently a Market Risk Manager at the Lloyds Banking Group, London, U.K. His research interests include power system operation, FACTS devices, and wind energy.

**Rodrigo Moreno** (M'05) received the B.Sc. and M.Sc. degrees from Pontificia Universidad Católica de Chile, Santiago, Chile, and the Ph.D. degree from the Imperial College, London, U.K. He is currently an Assistant Professor at the University of Chile and a Research Associate at Imperial College. His research interests include power system optimization, reliability and economics, renewable energy, and the smart grid.

**Goran Strbac** (M'95) is a Professor of electrical energy systems at Imperial College, London, U.K. His current research interests include electricity generation, transmission and distribution operation, planning and pricing, and integration of renewable and distributed generation in electricity systems.

**Diego Alvarado** received the B.Sc. degree in electrical engineering from the University of Chile, Santiago, Chile, in 2016. He is currently working toward the M.Sc. degree in electrical engineering at the University of Chile. His research interests include power systems economics, operation, and planning.